Multipactor discharge in a rectangular waveguide with regard to normal and tangential velocity components of secondary electrons

V.D. Shemelin[*],
Laboratory of Nuclear Studies, Cornell University, Ithaca, NY 14853

Abstract

The distributions of normal and tangential components of secondary electron velocity are found from known experimental data. These distributions are used for calculation of position, width and relative intensity of multipactor discharges zones. The calculations are performed for the vacuum waveguide of the CESR RF system.

1. Introduction

The problem on boundaries of multipactor discharge existence zones is encountered frequently in RF devices. Zones of the discharge were calculated in paper [1] for the case of parallel electrodes with consideration of real distribution of secondary electron energies. The angular distribution in space and possibility of return of the secondary electrons to the emitting electrode were also taken into account. A comparison with previously obtained experimental data confirmed validity of the analysis.

Recently two papers have appeared in connection with the problem of multipactor in a waveguide delivering power to a resonator [2, 3]. Influence of the own magnetic field of the wave on the motion of discharge electrons was taken into account in these articles. Also, the case when part of the power is reflected from the load, i.e. the standing wave exists, was examined. Because of supposed complexity of the motion in such conditions, the problem was solved by numerical simulations. Probe particles were launched at different initial phases into the gap. According to results of calculations of their energies and phases at the moment of impact to the wall, the conclusion was made about building-up or damping-out of the discharge.

A consideration of influence of the resonant cavity inherent magnetic field on the motion of particles in it was done in the article [4]. The radial drift of electrons moving parallel to axis in the axially symmetric cavity was analytically taken into account and the existence of the radial drift associated with RF magnetic field of the cavity was experimentally confirmed in that work.

The approaches described in [1] and [4] are used in the present paper for calculation of borders of the resonant RF discharge in a rectangular waveguide. It is shown that transverse (relative to the electric field) motion of secondary electrons can be related not only to the magnetic field but also to the initial velocity component parallel to electrode surface. It is proposed to analyze these two causes of drift separately. In the present article the drift related to the initial transverse velocities is discussed. Dimensions of the vacuum waveguide part of the CESR RF system and its operational frequency are used for illustration of results.

[*] Email: vs65@cornell.edu

2. Borders of discharge zones

Let us write the equation of motion for an electron in the gap as

$$\ddot{y} = \frac{eU}{md}\sin\omega t\,,$$

where the coordinate *y* is measured normal to the surface of one of the electrodes; *e/m* is the specific charge of the electron, this charge is considered positive to simplify the writing; *U* is the voltage amplitude across the gap *d*; $\omega = 2\pi f$, where *f* is the oscillation frequency; *t* is the time. It is useful to rewrite this equation in the normalized form:

$$\lambda'' = \xi\sin\theta\,, \tag{1}$$

where $\lambda = y/d,$ $\xi = U/U_0,$ $U_0 = m\omega^2 d^2/e,$ and $\theta = \omega t$; primes denote derivatives with respect to θ, while dots indicate derivatives with respect to *t*.

Integrating Eq. (1) we obtain

$$\lambda' = \xi(\cos\theta_1 - \cos\theta) + \beta_1\,, \tag{2}$$

$$\lambda = \xi(\theta - \theta_1)\cos\theta_1 + \xi(\sin\theta_1 - \sin\theta) + \beta_1(\theta - \theta_1)\,. \tag{3}$$

Here, θ_1 is the phase at which the electron enters the gap, and $\beta_1 = \bar{v}/\omega d$ is the dimensionless normal component of the initial velocity of the secondary electron.

A stable phase motion of the discharge particles is possible in the definite interval of initial phases, i.e. of phases when secondary particles enter the gap. These phases are calculated in [1] and can be expressed as follows:

for the lower boundary of the voltage

$$\theta_{1low} = \mathrm{atan}\left[2/(2n-1)\pi\right], \tag{4}$$

for the upper boundary of the voltage

$$\theta_{1up} = -\mathrm{atan}\frac{2}{(2n-1)\pi + \beta_1\left[4 - (2n-1)^2\pi^2\right]}. \tag{5}$$

Here, *n* is the order of multipactor, defined from the equation

$$\theta_2 - \theta_1 = (2n-1)\pi\,, \tag{6}$$

where $\theta_2 - \theta_1$ is a phase difference necessary for electron to cross the gap, so electron crosses the gap in an odd number of half-periods. Taking $\lambda = 1$ in (3) and using the condition of "resonance" (6) one can calculate the values of normalized voltage ξ. The lower and the upper values of RF voltage amplitude applied to the gap correspond to the values θ_1 taken from (4) and (5). One more variable in these formulas, β_1, as it is shown in [1], can be found from $\beta_1 = (2/3)\sqrt{2\overline{U}_s/U_0}$, where $\overline{U}_s$ is the voltage corresponding to the average initial velocity of the secondary electrons. It was found experimentally that for copper, for example, this average velocity corresponds to energy about 4 eV for a wide range of primary electron energies [5]. The normal component of the velocity according to [1] corresponds in this case to $(2/3)^2\overline{U}_s \approx 2$ Volts*.

* Generally, the mean value of velocity $\bar{v}$ and the square root from the mean value of the velocity square $\sqrt{\overline{v^2}}$ do not coincide. It can be shown, however, that in the case of rectangular distribution of the velocity

A particle with a negative phase at the entrance into the gap can return back to the electrode that emitted it. This gives base to some authors to examine only positive entrance phases. But it can be shown that the borders of discharge zones are significantly wider, namely thanks to negative phases at the entrance into the gap.

In the article [1] the motion of particles was analyzed for negative phases, and equations were obtained to find the limiting negative initial phases. For positive initial phases the same stability condition was used that was obtained earlier (the article [1] contains more detailed list of references for earlier works).

The limiting entrance phases, defined both by stability conditions and by the return of particles, are shown in Fig. 1. The figure presents only first two zones because it would be cumbersome to present all the data for a wide range of *fd* in one picture. For the CESR waveguide with cross-section of $17'' \times 4''$ the limiting phases are presented in the Table 1. One can see that for this value of *fd* the condition of return defines the border of discharge zone for the first order zone only.

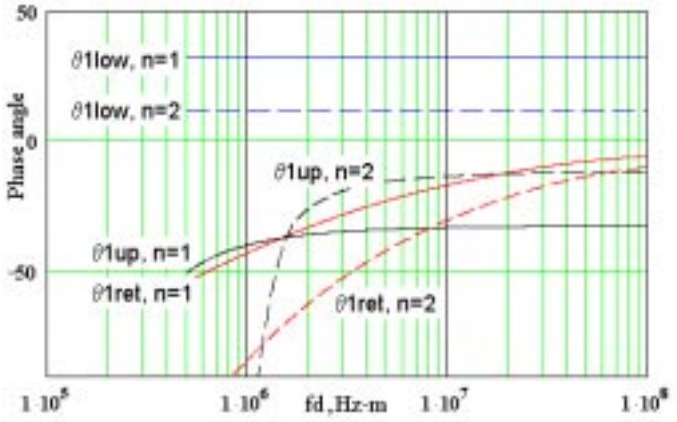

Fig. 1. Limiting entrance phases θ_1 for the 1st and the 2nd order of multipactor. The limits are shown for lower voltage of the zone (low), for upper voltage of the zone (up) (both defined by stability), and for the return (ret) condition of the motion.

---

squares, $\bar{v} = F(k)\sqrt{\overline{v^2}}$, where *k* is defined from $v_1 = kv_2$, v_1^2 and v_2^2 are minimal and maximal values in the distribution like in Fig. 3, but for velocity squares. $F(k) = \frac{2}{3} \cdot \frac{1+k+k^2}{1+k} \sqrt{\frac{2}{1+k^2}}$. When *k* runs from 0 to 1, $F(k)$ changes from $2\sqrt{2}/3 \approx 0.943$ to 1. The mean normalized velocity $\beta = \bar{v}_\perp / \omega d$, as indicated in [1] and discussed later, may be presented by $\beta = \frac{2}{3} \cdot \bar{v} / \omega d$. Taking into account limits of $F(k)$ and definitions made above for the equation of motion one can see that value of β can change between $0.943 \cdot \frac{2}{3}\sqrt{\frac{2\overline{U}_s}{U_0}}$ and $\frac{2}{3}\sqrt{\frac{2\overline{U}_s}{U_0}}$, i.e. between $\sqrt{\frac{2(0.395 \cdot \overline{U}_s)}{U_0}}$ and $\sqrt{\frac{2(0.444 \cdot \overline{U}_s)}{U_0}}$.

So, the difference between $\bar{v}$ and $\sqrt{\overline{v^2}}$ is not very big and assumed value of $\overline{U}_s$ (2 V) is good within 30 % in the worst case $(0.5/0.395 \approx 1.3)$.

Table 1. A case of CESR: $fd = 5.08 \cdot 10^7$ Hz·m, $f = 500$ MHz, $d = 4''$.

n	θ_{1low}, degrees	θ_{1up}, degrees	θ_{1ret}, degrees	W_{low}, eV	W_{up}, eV
1	32.48	-32.60	-7.88	59200	330000
2	11.98	-12.25	-13.91	11700	14000
3	7.26	-7.54	-18.06	4370	4670
4	5.20	-5.49	-21.42	2230	2310
5	4.05	-4.35	-24.33	1340	1360
6	3.31	-3.62	-26.92	883	895
7	2.80	-3.12	-29.28	623.2	629.2
8	2.43	-2.75	-31.46	461.0	464.3
9	2.14	-2.47	-33.50	353.2	355.2
10	1.92	-2.25	-35.43	278.2	279.5
11	1.74	-2.08	…	224.04	224.87
12	1.59	-1.93		183.67	184.24
13	1.46	-1.81		152.85	153.24
14	1.35	-1.71		128.81	129.10
15	1.26	-1.62		109.74	109.95
16	1.18	-1.55		94.37	94.53
17	1.11	-1.49		81.82	81.94
18	1.04	-1.43		71.45	71.54
19	0.99	-1.38		62.79	62.86
20	0.94	-1.34		55.49	55.55
21	0.94	-1.31		49.30	49.34
22	0.89	-1.27		43.99	44.03
23	0.85	-1.25		39.42	39.45
24	0.78	-1.22		35.46	35.49
25	0.74	-1.20		32.01	32.03

Other limiting reason for the discharge zone borders is energy. In order for the discharge to grow, the energy of the incident electrons must be such that the secondary emission coefficient (SEC) is greater than 1. For a carefully cleaned copper surface, SEC > 1 in the energy interval 200 ÷ 1500 eV; however, in practice the copper surface is often impure, in which case the interval is enlarged to 70 ÷ 2300 eV, and the maximum of the SEC shifts from 600 to 200 eV [5, 6, 7]. Some authors use different approximation for dependence of SEC on energy [8]:

$$\delta(u) = \delta_m \cdot \frac{1 - \exp\left[-A(u/u_m)^B\right]}{C(u/u_m)^D}, \tag{7}$$

where u is the impact energy of the primary electron and $\delta_m = 1.6$ is the maximum SEC corresponding to an impact energy of $u_m = 200$ eV. The curve fitting parameters are A = 1.55, B = 0.9, C = 0.79, and D = 0.35. This formula gives even worse case for the small energy electrons, because δ becomes less than 1 at the energy only less than 33 eV. We will use this formula here for more straightforward comparison with the results of [3]. The energy of incident electrons can be obtained from (2), allowing the condition of "resonance" (6):

$$W = \frac{mv^2}{2} = \frac{m}{2}(\lambda' \omega d)^2 = \frac{eU_0}{2}(2\xi \cos\theta_1 + \beta_1)^2 .$$

Taking as θ_1 in this formula the values of θ_{1low} and θ_{1up} from (4) and (5) we obtain W_{low} and W_{up} - the energies at the lower and the upper boundaries of the discharge zones, they are also presented in the Table 1.

Zones of multipactor are presented in Fig. 2 in accordance to stability condition with limiting angles taken from Table 1. The heights of the columns are proportional to $\delta(W_{low}) \approx \delta(W_{up})$. Only zones with $\delta > 1$, when the discharge exists, are shown. The voltage across the gap is taken at the middle plane of the waveguide with a traveling wave. We do not consider the influence of the magnetic field and existence of a wide range of voltages across the broad side of the waveguide with a mode TE_{10}. It is supposed that the discharge exists in the area close to the middle plane of the waveguide. This assumption has no explanations in frames of presented model but the results of simulations [3] support it well with respect to position of most zones. This analytical model is "free of noise" that is inherent to the simulation, and takes much less time for calculation. Besides, this model shows the position of some zones that were not indicated in the cited work. The narrowest zones could not be revealed by simulation because of discrete set of starting phases used or can be inhibited by the magnetic field.

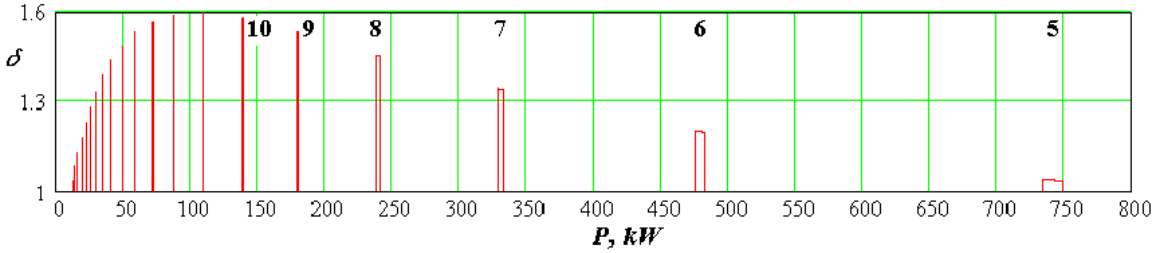

Fig. 2. Multipactor zones for traveling wave in the CESR B-cell waveguide (17″× 4″) allowing for normal only components of initial velocities.

There is one more reason why the narrowest zones of the discharge should not exist in reality. The presence of the tangential velocity component brings about the shift of electrons trajectories with respect to the surface normal even if there is no magnetic field.

3. Distribution of normal and tangential components of the secondary electron (SE) velocities

a) Determination of $\bar{v}_\perp$.

The angular distribution of the SE is described by a polar diagram [5], which is nearly circular, i.e. almost cosinusoidal:

$$dn/n \propto \cos\varphi d\Omega,$$

where φ is the angle between the velocity vector of the secondary electrons and the normal to the surface, and $d\Omega$ is the element of solid angle.

Since $d\Omega = 2\pi \sin\varphi d\varphi$, we have $dn/n \propto 2\pi \sin\varphi\cos\varphi d\varphi$.

After normalization, because $\int dn/n = 1$, one can obtain

$$dn/n = 2\sin\varphi\cos\varphi d\varphi. \qquad (8)$$

Now let us bring in the velocity distribution of SE. The actual distribution function is rather complicated, so, for the beginning, let this function has a rectangular shape (Fig. 3):

$$f(v)=\begin{cases}0, & v<v_1\\ \dfrac{1}{v_2-v_1}, & v_1\le v\le v_2\\ 0, & v>v_2\end{cases} \tag{9}$$

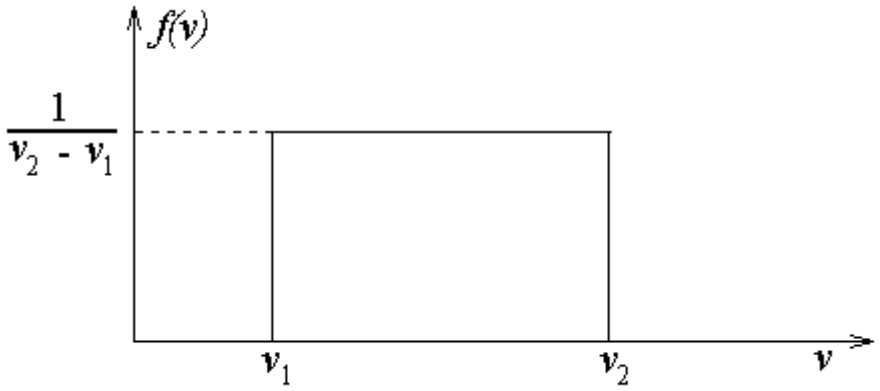

Fig. 3. Rectangular distribution of SE velocities.

The number of SE outgoing into the angle between φ and $\varphi+d\varphi$ and having the normal velocity component within the interval from $v_\perp$ to $v_\perp+dv_\perp$, one can write as

$$dn'_\perp = dn\cdot f(v')dv', \tag{10}$$

where *dn* is taken from (8) and $v'=v_\perp/\cos\varphi$.

Using (8) and (9) we can write

$$\frac{dn'_\perp}{n}=2\sin\varphi\cos\varphi\cdot f\left(\frac{v_\perp}{\cos\varphi}\right)\frac{dv_\perp d\varphi}{\cos\varphi},$$

so that

$$dn_\perp/n = 2dv_\perp\int f\left(v_\perp/\cos\varphi\right)\sin\varphi d\varphi\,. \tag{11}$$

$dn'_\perp$ differs from $dn_\perp$ by the following: $dn'_\perp$ is the number of electrons with normal velocity component $v_\perp \div v_\perp+dv_\perp$ within the angle $\varphi\div\varphi+d\varphi$, $dn_\perp$ is the number of electrons with components $v_\perp\div v_\perp+dv_\perp$ with any angle of take-off.

In the integral (11) we have to take as limits of integration those values of φ where the function $f\left(v_\perp/\cos\varphi\right)$ is not zero. So we have (Fig. 4)

$$\frac{dn_\perp}{n} = 2dv_\perp \begin{cases} \int_{v_\perp/v_2}^{v_\perp/v_1} \frac{1}{v_2 - v_1} \cdot d(\cos\varphi), & 0 < v_\perp < v_1 \\ \int_{v_\perp/v_2}^{1} \frac{1}{v_2 - v_1} \cdot d(\cos\varphi), & v_1 \le v_\perp \le v_2 \end{cases}$$

$$= 2dv_\perp \begin{cases} \frac{1}{v_2 - v_1} \cdot \left(\frac{v_\perp}{v_1} - \frac{v_\perp}{v_2} \right) = \frac{v_\perp}{v_1 v_2}, & 0 < v_\perp < v_1 \\ \frac{1}{v_2 - v_1} \cdot \left(1 - \frac{v_\perp}{v_2} \right), & v_1 \le v_\perp \le v_2 \end{cases} \qquad (12)$$

Graphically this distribution is presented in Fig. 5.

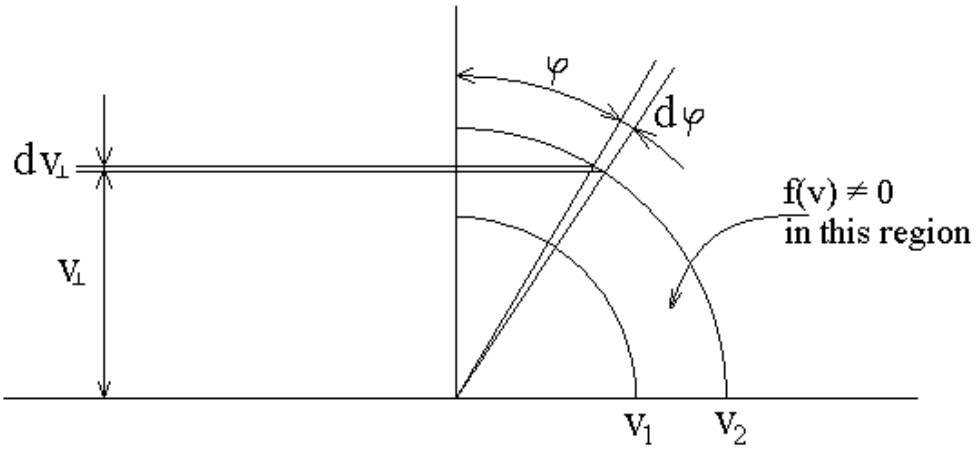

Fig. 4. For calculation of $v_\perp$.

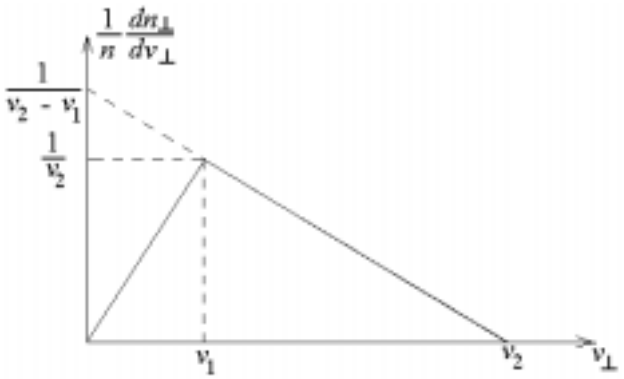

Fig. 5. Distribution function for velocity normal component (the same for tangential).

Now it is easy to calculate $\bar{v}_\perp$:

$$\bar{v}_\perp = \int v_\perp \cdot \frac{dn_\perp}{n} = \int_0^{v_1} \frac{2v_\perp^2 dv_\perp}{v_1 v_2} + \int_{v_1}^{v_2} \frac{2v_\perp dv_\perp}{v_2 - v_1} - \int_0^{v_1} \frac{2v_\perp^2 dv_\perp}{v_2(v_2 - v_1)} = \frac{v_1 + v_2}{3}.$$

Since $\bar{v} = \frac{v_1 + v_2}{2}$, we have $\bar{v}_\perp = \frac{2}{3}\bar{v}$.

Since any function can be presented as a superposition of rectangular functions, the last statement is a general one.

b) Determination of $\bar{v}_\parallel$.

The number of SE outgoing into the angle between φ and $\varphi + d\varphi$ and having the tangential velocity component within the interval from $v_\parallel$ to $v_\parallel + dv_\parallel$ one can write as

$$dn'_\parallel = dn \cdot f(v'')dv'', \tag{13}$$

where $v'' = v_\parallel / \sin\varphi$; $f(v)$, the same as above, is the velocity distribution function for SE.

Let us integrate $dn'_\parallel$ in respect to angle to obtain the distribution function for the velocity component tangential to surface: $dn_\parallel / n$.

From (7) and (12) we obtain

$$dn_\parallel / n = 2dv_\parallel \int f\left(v_\parallel / \sin\varphi\right)\cos\varphi d\varphi . \tag{14}$$

As before for $\bar{v}_\perp$ we have to take the limits of integration so that the function $f\left(v_\parallel / \sin\varphi\right)$ is not zero (Fig. 6):

$$\frac{dn_\parallel}{n} = 2dv_\parallel \begin{cases} \int\limits_{v_\parallel/v_2}^{v_\parallel/v_1} \frac{1}{v_2 - v_1} \cdot d(\sin\varphi), & 0 < v_\parallel < v_1 \\ \int\limits_{v_\parallel/v_2}^{1} \frac{1}{v_2 - v_1} \cdot d(\sin\varphi), & v_1 \le v_\parallel \le v_2. \end{cases}$$

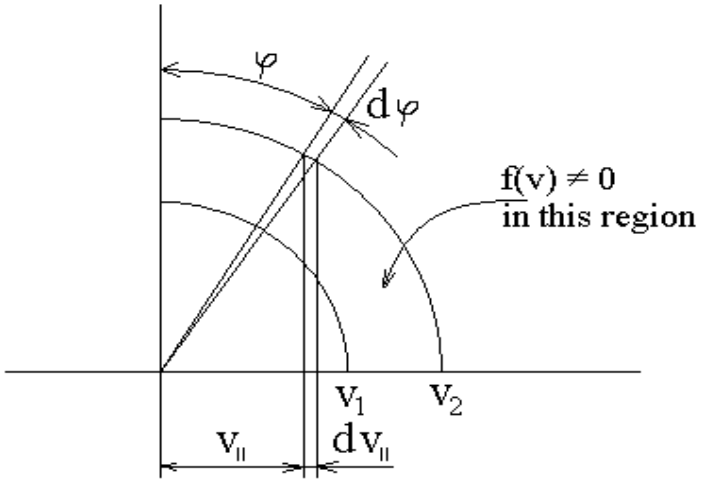

Fig. 6. For calculation of $v_\parallel$.

One can see that integrals in the last expression differ from (12) by designation of the integration variable only. So, all the previous results for $\bar{v}_\perp$ are valid for $\bar{v}_\parallel$:

$$\bar{v}_{\perp} = \bar{v}_{\parallel}, \qquad \bar{v}_{\parallel} = \frac{2}{3}\bar{v}.$$

The distribution function for $\bar{v}_{\parallel}$ is the same as for $\bar{v}_{\perp}$ (Fig. 5).

4. Transverse motion of electrons due to tangential component of initial velocity

Knowing the mean value of module of tangential to surface velocity component, we can find the mean value of the module of this component along the arbitrary selected direction *x*. The problem can be reduced to the calculation of mean value of cosine when the angle changes between 0 and $\pi/2$:

$$\bar{v}_x = \overline{v_{\parallel} \cdot \cos\alpha} = \bar{v}_{\parallel} \cdot \overline{\cos\alpha}.$$

Designating $\overline{\cos\alpha}$ as $\bar{c}$, we have

$$\bar{c} = \overline{\cos\alpha} = \frac{2}{\pi}\int_0^{\pi/2} \cos\alpha d\alpha = \frac{2}{\pi},$$

because the angle distribution is homogeneous.

The mean shift along the *x*-axis for one flight of the multipactor electron across the gap can be written now as

$$\bar{X}_1 = \bar{c} \cdot v_{\parallel} \cdot \frac{(2n-1)T}{2}.$$

Since $\beta_1 = \frac{\bar{v}_{\perp}}{\omega d} = \frac{\bar{v}_{\parallel}}{\omega d} = \frac{2}{3}\sqrt{2\bar{U}_s / U_0}$, we have $\bar{X}_1 = \frac{4}{3}(2n-1)\sqrt{\frac{2\bar{U}_s}{U_0}} \cdot d$. (15)

After *N* flights across the gap the multipactor electron will shift along the *x*-axis by the mean distance

$$\bar{X}_N = \frac{4}{3}(2n-1)\sqrt{N}\sqrt{\frac{2\bar{U}_s}{U_0}} \cdot d.$$

Now the question arises: under what conditions the discharge can keep burning in the region where the voltage is within boundary values and the secondary emission coefficient (SEC) is more than 1, but some particles drift away from this region permanently?

Let us assume that in the central part of the waveguide with a traveling wave the voltage is equal to the maximal limit voltage of the discharge U_{up}. At some distance X_{low} from the middle plane the voltage corresponds to the minimal discharge voltage U_{low}. Let us suggest that on the border of this region two electrons are launched. After random side shifts that occur by each flight across the gap, one half of descendants of these electrons will come into zone of stability and another half will go out into the opposite direction. The electrons that came into the zone of stability will reach *on average* the other border of the zone by the number of flights equal to *N*, and

$$2X_{low} = \sqrt{N} \cdot \bar{X}_1 \qquad (16)$$

If, at the other border of the zone 2 electrons *on average* appear, the situation is repeated: one half of their descendants will go into the stability zone and another half will not go into it.

So, the condition of self-supporting discharge $\delta > 1$ in the presence of losses is changed to

$$\delta^N > 2. \tag{17}$$

X_{low} can be found from the condition

$$U_{low} = U_{up} \cos\frac{\pi X_{low}}{a},$$

where U_{up} is the voltage at the field maximum, a is the width of the waveguide. Changing to normalized voltages, we can write

$$\frac{U_{low}}{U_{up}} = \frac{\xi_{low}}{\xi_{up}} = \cos\frac{\pi X_{low}}{a}.$$

ξ_{low} and ξ_{up}, as is shown in [1], for the "resonant" motion are equal to

$$\xi = \frac{1-(2n-1)\pi\beta_1}{(2n-1)\pi\cos\theta_1 + 2\sin\theta_1},$$

where θ_1 for ξ_{low} should be taken from (4) and for ξ_{up} - from (5). So

$$\cos\frac{\pi X_{low}}{a} = \frac{1+\dfrac{2}{(2n-1)\pi}\tan\theta_{1up}}{1+\dfrac{2}{(2n-1)\pi}\tan\theta_{1low}}, \tag{18}$$

where $\tan\theta_{1low} = \dfrac{2}{(2n-1)\pi}$, $\tan\theta_{1up} = -\dfrac{2}{(2n-1)\pi + \beta_1\left[4-(2n-1)^2\pi^2\right]}$.

Substituting X_{low} from (16) and $\overline{X}_1$ from (15) into (18), we obtain

$$N = \left[\frac{\arccos\left[\dfrac{(2n-1)\pi + 2\tan\theta_{1up}}{(2n-1)\pi + 2\tan\theta_{1low}}\right]}{\dfrac{2\pi}{3}(2n-1)\dfrac{d}{a}\sqrt{\dfrac{2\overline{U}_s}{U_0}}}\right]^2. \tag{19}$$

The obtained number of impacts N is a function of the zone number n. The SEC is also a function of the zone number because in the limits of the zone the energy of primary electrons weakly depends on the initial phase, at least for zones with the number more than $n = 4$ (Table 1).

Let us define the effective SEC as

$$\delta_{eff} = \delta \cdot 2^{-1/N}.$$

The number of particles within the stability zone after N acts of multiplication is equal to

$$\delta_{eff}^N = \delta^N / 2,$$

so to support the discharge it is necessary, like in the absence of losses, that

$$\delta_{eff} > 1.$$

The value of δ_{eff} reflects the rate of development of the discharge, so as δ in the absence of losses.

Let us calculate N, δ and δ_{eff} for values of n = 4, 5, …, 13. For calculation of δ we shall use the formula (7) and values of energy from Table 1. Results of calculations are brought together in Table 2.

Table 2. δ_{eff} for the CESR B-cell waveguide (500 MHz, 17″×4″).

n	δ	N	δ^N	δ_{eff}
4	0.865	206	$1\cdot10^{-13}$	0.863
5	1.038	76.2	17.0	1.029
6	1.198	34.5	512	1.175
7	1.341	18.2	187	1.289
8	1.454	10.2	44.9	1.358
9	1.534	6.2	14.3	1.372
10	1.580	4.0	6.3	1.330
11	1.597	2.7	4.0	1.238
12	1.590	1.9	2.4	1.107
13	1.566	1.4	1.9	0.950

For the case when the voltage amplitude in the middle plane of the waveguide U_m is in the interval $U_{low} < U_m < U_{up}$, the space zone of the multipactor becomes narrower. The minimal value of U_m, at which the discharge is still possible, will be more than U_{low}. In this case $\delta_{eff} = 1$. We can find the value of U_m from conditions analogous to (18):

$$\cos\frac{\pi X_{low}}{a} = \frac{1+\dfrac{2}{(2n-1)\pi}\tan\theta_{1m}}{1+\dfrac{2}{(2n-1)\pi}\tan\theta_{1low}},$$

using N like in (19) but with θ_{1m} instead of θ_{1up} and $\delta^N = 2$.

Multipactor zones with taking into account scattering related to the spread of tangential velocities are presented in Fig. 7 for the waveguide with cross-section of 17×4 inches^2. Comparison with Fig. 2 shows significant decrease of the number of possible zones and of their intensity.

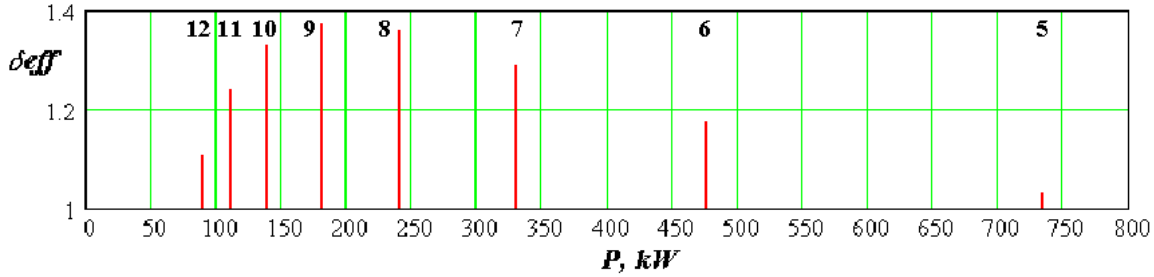

Fig. 7. Positions and intensity of multipactor zones allowing for initial tangential and normal velocities. Traveling wave 500 MHz, 17″×4″ waveguide.

5. Conclusion

Zones of the multipactor discharge in a rectangular waveguide are calculated. Non–zero normal component of initial velocity of secondary electrons leads to possibility of starting at retarding phases and so to widening of discharge zones. The distributions of normal and tangential electron velocities are found from the experimentally known cosine angular distribution of velocities and the energy distribution. It is shown that existence of transverse component of initial velocity leads to significant losses of secondary electrons and reduces possible multipactor zones both in number and intensity. The model of random wandering is used for taking into account escaping of electrons from the stability zone. For this case the conception of effective secondary emission coefficient is introduced.

The real width and intensity of discharge zones should be expected to be somewhere in the middle of analyzed cases – with regard to transverse scattering of electrons and without. This is due to suppression of scattering and to the drift of electrons to the middle plane of the waveguide because of the wave own magnetic field.

Calculations are performed for the vacuum waveguide of the 500 MHz CESR superconducting cavity.

6. Acknowledgments

The author is grateful to Sergey Belomestnykh for numerous fruitful discussions and careful reading of the manuscript, and Hasan Padamsee for initiating this work.

References

1. *V.D. Shemelin*. Existence zones for multipactor discharges. Sov. Phys. Tech. Phys. **31** (9), September 1986.

2. *E. Chojnacki*. Simulation of multipactor-inhibited waveguide geometry. Phys. Rev. ST Accel. Beams **3**, 032001 (2000).

3. *R.L. Geng, H.S. Padamsee*. Exploring multipacting characteristics of a rectangular waveguide. Proceedings of the 1999 Particle Accelerator Conference, vol. I, pp. 429 – 431. New York, NY.

4. *V.D. Shemelin.* Effect of the intrinsic magnetic field of a volume resonator on the secondary electron discharge in it. Journal of Applied Mechanics and Technical Physics. 1981. Translation from Russian. 1982 Plenum Publishing Corporation.

5. *I.M. Bronshtein and S.M. Fraiman*. Secondary electron emission (in Russian). Nauka, Moscow, 1969, p. 407.

6. *N.O. Chechik, S.M. Fainshtein, and T.M. Lifshits*. Electron multiplier tubes (in Russian). GITTL, Moscow, 1957, p. 575.

7. *H. Bruining.* Physics and applications of secondary electron emission. McGraw-Hill, New York, 1954.

8. *G.E. Dionne.* Origin of secondary-electron-emission yield-curve parameters. J. Appl. Phys. **46**, 3347, 1975.